ACS APPLIED MATERIALS & INTERFACES

Research Article

www.acsami.org

Development of Antimicrobial Coatings by Atmospheric Pressure Plasma Using a Guanidine-Based Precursor

Jacqueline H. Yim, Michelle S. Fleischman, Victor Rodriguez-Santiago,* Lars T. Piehler, André A. Williams, Julia L. Leadore, and Daphne D. Pappas

U.S. Army Research Laboratory, Weapons and Materials Research Directorate, Aberdeen Proving Ground, Maryland 21005, United States

ABSTRACT: Antimicrobial coatings deposited onto ultra high molecular weight polyethylene (UHMWPE) films were investigated using an atmospheric pressure - plasma enhanced chemical vapor deposition (AP-PECVD) process. Varying concentrations of a guanidine-based liquid precursor, 1,1,3,3-tetramethylguanidine, were used, and different deposition conditions were studied. Attenuated total reflectance - Fourier Transform Infrared (ATR-FTIR) spectroscopy and X-ray Photoelectron Spectroscopy (XPS) were used to study the chemical structure and elemental composition of the coatings. Conformity, morphology, and coating thickness were assessed through SEM and AFM. Optimal AP-PECVD parameters were chosen and applied to deposit guanidine coatings onto woven fabrics. The coatings exhibited high antimicrobial activity against *Escherichia coli* (*E. coli*) and *Staphylococcus aureus* (*S. aureus*) based on a modified-AATCC 100 test standard, where 2−5 log reductions were achieved.

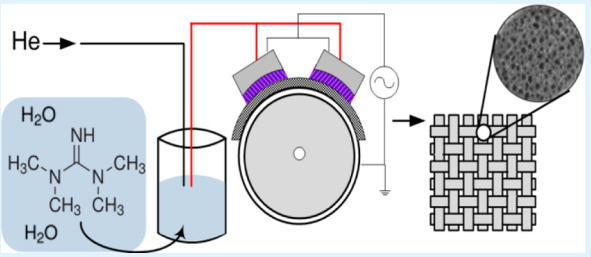

KEYWORDS: *guanidine, antimicrobial, atmospheric pressure plasma, plasma enhanced-chemical vapor deposition, ultra high molecular weight polyethylene (UHMWPE), textiles*

1. INTRODUCTION

Polymers and salts synthesized from guanidine and its derivatives have been reported to demonstrate excellent antimicrobial and biocidal properties owing to the highly cationic nature of the compound. The antimicrobial mechanism of guanidines is believed to proceed through electrostatic interactions at the bacteria or organism cell membrane, similar to the mechanisms associated with cationic surface-active microbiocides such as quaternary salts, long-chain aliphatic alkyl amines, etc.[1,2] The attraction between positively charged ions of the antimicrobial agent with that of the negatively charged surface of the microbial cell disrupts or imposes a charge imbalance, thus triggering the breakdown of the cell membrane and leading to the leakage of intracellular contents. Due to their broad-spectrum of antimicrobial activity and low toxicity, guanidine polymeric derivatives have found applications in the medical,[3] cosmetic,[4] textile,[5] and food industries.[6]

Polymeric guanidine derivatives that have been synthesized and reported have been largely accomplished via polymerization reactions, usually involving the use of guanidine salts and monomers[7,8] and other synthetic wet chemistry routes.[9] Rather than pursuing similar wet-chemistry routes, other methods used to deposit coatings have been considered based on processing merits. One such technique utilizes nonequilibrium plasmas. Conventionally, low pressure plasmas have produced conformal polymeric coatings.[10−12] However, in recent years, the use of atmospheric pressure plasmas has gained more interest over low pressure systems owing to ease of processing (no vacuum equipment required) and scalability. Atmospheric pressure plasmas have been utilized in the engineering of antimicrobial materials, where their applications ranged from surface pretreatment of substrates for enhanced bonding of silver nanoparticles or antimicrobial agents in imparting antimicrobial behavior on surfaces spanning from pretreatments of substrate materials[13,14] and very recently, deposition and/or plasma polymerization of antimicrobial polymers using monomer precursors.[15−18]

In this study, we investigated the use of an atmospheric pressure-plasma enhanced chemical vapor deposition (AP-PECVD) process to develop coatings from a guanidine-derived monomer, 1,1,3,3-tetramethylguanidine (TMG), that impart antimicrobial behavior onto polymeric substrates. To our knowledge, efforts to deposit a guanidine-based polymer coating using the specified precursor with an atmospheric pressure plasma source have not been taken or cited in the literature. The work presented focuses on the characterization of the AP-PECVD coatings and correlating chemical and physical properties and antimicrobial efficiency to deposition conditions.

2. EXPERIMENTAL SECTION

2.1. Atmospheric Pressure Plasma Enhanced Chemical Vapor Deposition (AP-PECVD). Depositions were carried out using an APC 2000 dielectric barrier discharge (DBD) plasma system

Received: August 20, 2013
Accepted: October 29, 2013
Published: October 29, 2013

(Sigma Technologies Intl. Inc.) in a cylindrical roller configuration, as shown in Figure 1. The roller component consists of an electrode

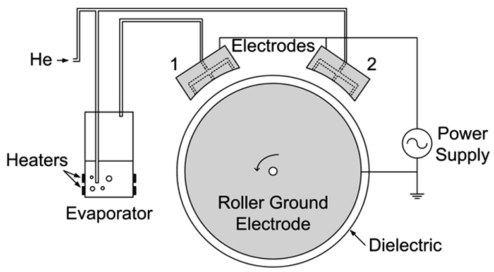

Figure 1. RF cylindrical atmospheric pressure plasma setup.

covered with an alumina dielectric that acts as the ground and two high voltage (HV) electrode plates (45.72 × 5.72 cm per plate) positioned above the roller. The electrodes have slit channels along their length to allow gas to diffuse through. An interelectrode gap distance of 2 mm was used throughout all treatments. The DBD plasma reactor is equipped with a radio-frequency (RF) power supply that operates at 90 kHz, yielding a power density of 0.57−0.62 W·cm^{-2}, corresponding to a power of 300−330 Watts.

A 6.5 L stainless steel evaporator connected to the gas handling system of the setup was used for the conversion of liquid precursors placed in it to a vapor form. The carrier gas, helium, used in the AP-PECVD process was fed to the evaporator containing the precursor and administered to the HV electrodes through gas feed lines 1 and 2. The evaporator was set at a constant temperature of 25 °C, and a fixed helium flow-rate of 14,000 sccm was used throughout. Deposition times of 30, 60, and 180 seconds were implemented.

2.2. Materials. Ultra high molecular weight polyethylene (UHMWPE) films with a thickness of 75 μm (Goodfellow Co.) served as the model polymer substrate used to deposit and characterize properties of the coatings. Prior to deposition, the films were cleaned in ethanol and dried in open air. The antimicrobial agent, 1,1,3,3-tetramethylguanidine (TMG) (99%, Aldrich), was used as received. TMG solutions used in the deposition process included 1.0, 5.0, and 10.0% (w/w) of TMG in deionized water (Milli-Q, 18 MΩ•cm) and were used to study the role of precursor concentration on the composition of the as-deposited coatings. The feasibility of depositing the guanidine-based coating onto woven fabrics was investigated using Spectra (scoured Spectra 1330, Honeywell), an ultra high molecular weight polyethylene woven fabric, and nylon/cotton blend woven fiber mats.

2.3. Characterization of Coatings. Attenuated total reflectance - Fourier Transform Infrared Spectroscopy (ATR-FTIR) was utilized to study the chemical composition of each coating. Spectra were recorded using a Thermo-Nicolet Nexus 870 FT-IR spectrometer equipped with a Thermo-Nicolet OMNI-Sampler ATR accessory, a single-bounce HATR Germanium crystal. A deuterated triglycine sulfate (DTGS) and potassium bromide (KBr) beamsplitter was used. For each spectrum, 64 scans were collected at a resolution of 4 cm^{-1}.

In addition to ATR-FTIR, near-surface compositional depth profiling of the as-deposited coatings was performed using a Kratos Axis Ultra X-ray photoelectron spectroscopy (XPS) system, equipped with a hemispherical analyzer. A 100 W monochromatic Al Kα (1486.7 eV) beam irradiated a 1 mm × 0.5 mm sampling area with a take-off angle of 90°. The base pressure in the XPS chamber was held between 10^{-9} and 10^{-10} Torr. Elemental high resolution scans for C_{1s}, N_{1s}, and O_{1s} were taken in the constant analyzer energy mode with 20 eV pass energy. For the binding energy calibration of the TMG coatings and the pristine UHMWPE C_{1s} spectra, 285.0 eV was used as the reference peak corresponding to the aliphatic carbon−carbon, C−C group. Deconvolution of high resolution C_{1s} spectra was done using the CasaXPS fitting software with a Gaussian-Lorentzian fit. A minimum of three sampling areas on the same sample were analyzed.

Atomic force microscopy (AFM) was used to study the morphology of the coatings and to assess the surface roughness. The AFM system used was a Dimension 3100 microscope with a Nanoscope V controller (Digital Instruments/Veeco). Imaging was done in tapping mode of 10 × 10 μm areas, using RTESP (silicon) cantilevers (Bruker) with an oscillation frequency of 300 kHz and a scan rate of 0.5 Hz. Using Nanoscope software (v7.30), images were first-order x−y plane fitted and then first-order flattened. Surface roughness measurements were based on root mean square (RMS) roughness values averaged from three images scanned at different locations on each sample. Surface morphology was also assessed using scanning probe microscopy (SEM). An FEI Nova NanoSEM operating in both field-emission and immersion modes under nominal accelerating voltages of 1−3 eV was additionally employed. All images were captured at a magnification of 20,000×.

Proton and ^{13}C NMR analysis were performed on a Bruker 600 MHz instrument. The NMR solvent used was deuterated acetone (acetone-d_6) containing a 1% v/v TMS internal standard. The water used in this study was purified by a Nanopure Infinity ultrapure water system.

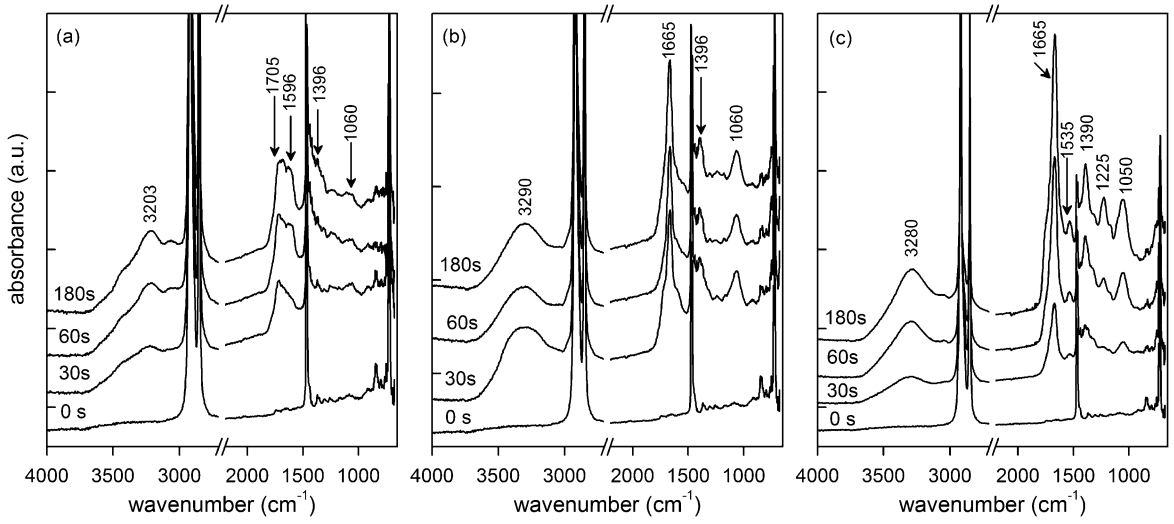

Figure 2. ATR-FTIR absorption spectra of an uncoated UHMWPE film and UHMWPE film with (a) 1% wt%, (b) 5 wt %, and (c) 10 wt % TMG coatings deposited after 30, 60, and 180 s.

2.4. Antimicrobial Testing. The antimicrobial performance of the TMG-derived coatings was tested against *E. coli* (Gram-negative) and *S. aureus* (Gram-positive) organisms using a modified AATCC Test Method 100 described by Sun et al.[19] This method allows the testing of fabrics with higher hydrophobicity as compared with the original standard. The procedure entails sandwiching the inoculums/organisms between two 2.5 × 2.5 cm^2 fabric swatches. Prior to testing, individual swatches were dipped in a 70/30 ethanol/water mixture and dried to remove any loosely bound physisorbed molecules and/or contaminants. Swatches of the textile fabric were inoculated with 100 μL of 10^6 cells/mL of *E. coli* and *S. aureus* and was sandwiched between the two parts (1 mL/100 mL Trypticase Soy broth), and a sterile 50 mL beaker were placed on top. The sample and beaker were contained in a sealed, sterile cup. All samples were incubated at 37 °C for two hours. Samples were recovered by removing the beaker and then adding 50 mL of sterile Dey-Engley broth. Samples were then sonicated for 1 min and vortexed for 1 min. Dilutions were made in sterile 0.85% NaCl water and plated in Trypticase Soy Agar plates. All testing was conducted in triplicates.

3. RESULTS AND DISCUSSION

3.1. Chemical Composition of AP-PECVD Guanidine Coatings. Various concentrations of 1,1,3,3-tetramethylguanidine solutions and deposition times were investigated in obtaining polymeric guanidine-derived coatings. From infrared absorption spectroscopy measurements, the addition of the TMG coatings on the UHMWPE film introduced new IR peaks. These absorption bands were identified and found to increase in intensity with deposition time and increased TMG concentration in the precursor solution. Vibrational stretching bands of the methylene groups, the main absorption peaks of the UHMWPE film, were present as well as new peaks that are representative of the chemistry of the coatings as seen in Figure 2. The assignment of these new peaks at their respective frequencies is summarized in Table 1, where amines, amides, carboxyl, and hydroxyl groups are among the main chemical constituents that make up the chemical structure of the coatings.

Table 1. Characteristic FTIR Absorption Frequencies Corresponding to Chemical Groups Found in TMG Coatings[22−24]

wavenumbers (cm^{-1})	functional group assignment
3290−3280, ∼3200	N−H str., amines or amides or O−H str. alcohol
1705	C═O str., aliphatic amide or carboxylic acid
1665	C═N str., aliphatic imines or oximes
1596	N−H def, primary amides
1535	N−H def., secondary amides
1396	C−O str., or O−H def., carboxyl
1300−1315	C−O str., carboxyl
1225	N−H def., secondary amides or C−N str., aliphatic amines
1050−1060	C−O str., sat aliphatic primary alcohols

The concentration of TMG in water plays a critical role in the chemical composition of the as-deposited coating and is made apparent from FTIR spectra. This is clearly illustrated by the appearance and absence of specific spectral bands found in the coatings deposited using the 1, 5, and 10 wt % TMG solutions. Prominent bands identified in the 1 wt % coatings were at ∼3200, 1705, 1596, and 1060 cm^{-1}, corresponding to the O−H stretching of an alcohol or N−H stretching of an amine, the C═O stretching band of an aliphatic amide or carboxylic acid, the N−H stretching of an amide, and the C−O stretching of hydroxyl groups, respectively. The addition of oxygen-containing functional groups was likely attributed to water vapor-plasma interactions in the plasma-assisted deposition process. OH, O, and O_2 metastable species and water cluster ions have been cited to dominate in the plasma depending on the water vapor concentration.[20] Similar results of oxidized polar groups such as hydroxyls, carbonyls, and carboxyl groups on the surfaces of UHMWPE films from water vapor plasma treatments have been reported by Rodriguez-Santiago et al.[21] Also, reactive species such as ozone, O_2, and O generated from plasma interactions with air from open atmosphere are also an underlying source of oxygen-bearing groups.

As the concentration of TMG in water increased to 5 and 10 wt %, the same peaks identified in the 1 wt % TMG coatings were found to be more pronounced and additional peaks were observed. The most distinctive absorption band was attributed to the imine group at 1665 cm^{-1}. Other identified groups include the N−H deformation band of primary amide, N−H deformation band of secondary amide, C−O or O−H deformation of carboxyl, C−O stretching of carboxyl, and N−H deformation of secondary amides or C−N stretching of amines at 1535, 1396, 1300−1315, and 1225 cm^{-1}, respectively. Drawing from FTIR spectral analyses, the 5 and 10 wt % TMG solutions yield a more amine-rich coating resembling the guanidine structure. Though the IR spectra for the 5 and 10 wt % TMG coatings are comprised of similar spectral bands, little change in the evolution of the peak intensity with deposition time was seen with the 5 wt % TMG coatings. This suggests that the coating retains the same chemical composition irrespective of deposition time. Furthermore, this alludes that the concentration of the TMG in the water yields a uniform deposition driven by reaction kinetics that are consistent with time in the plasma. Overall, the effect TMG concentration has on the composition and chemistry of the coatings suggests that concentration of TMG in solution is the limiting factor that governs the concentration of TMG fragmented chains that can partake in surface recombination reactions.

In addition to TMG concentration, deposition time was also found to influence the composition of the coatings. As deposition time increased, the intensity of absorption bands associated with the coatings also increased. This was mainly observed with peaks found in the 1000−1700 cm^{-1} and at 3200 cm^{-1}. The intensity of these bands signifies that fragmented segments of the TMG precursor and water vapor are incorporated or grafted onto the backbone of the polymeric coating with prolonged deposition time. Furthermore, the increase in peak heights, mainly the imine seen in the 5 and 10 wt % TMG coatings, suggests that there is a preferential attachment of this chemical group. This can also be an indication of increased film thickness with time.

X-ray photoelectron spectroscopy (XPS) was employed to study the chemical composition and reconfirm functional groups previously identified through FTIR of the grown films. However, it should be noted that the analysis depth is different for the two techniques, with XPS probing closer to the surface. From survey scans, the elemental composition of the 1, 5, and 10 wt % TMG coatings are summarized in Table 2. The observed atomic concentrations reveal that the coatings are highly oxidized with compositional make-up comprised of 17−20 at. % of oxygen and only 3−11 at. % of nitrogen. The highest concentration of oxygen groups were associated with

Table 2. Elemental Composition of TMG Coatings on UHMWPE Film Based on TMG Concentration and Deposition Time and Calculated Relative Ratios, N/C and O/C

		atomic concn (at. %)			relative ratio	
% TMG (w/w)	dep. time (s)	C	N	O	N/C	O/C
1	30	75.0	3.4	21.6	0.05	0.29
	60	72.7	4.2	23.1	0.06	0.32
	180	71.1	5.5	23.4	0.08	0.33
5	30	72.3	9.4	18.2	0.13	0.25
	60	73.2	9.1	17.7	0.13	0.24
	180	71.4	8.8	19.8	0.12	0.28
10	30	76.3	6.1	17.7	0.08	0.23
	60	74.6	7.3	18.2	0.10	0.24
	180	70.2	10.2	19.6	0.15	0.28

coatings derived from the 1 wt % TMG solution, where a 7% increase in the uptake of oxygen was observed. This was expected as the reactive species in the precursor vapor would be mainly comprised of water vapor rather than the TMG. In the case of the 5 and 10 wt % TMG coatings, the concentration of oxygen was reduced by 16−23% from that of the 1 wt % TMG coatings, and the nitrogen uptake was 2−3 times higher. A broader assessment of the atomic concentrations revealed that little to no change in compositional make-up of the coatings occurs by varying deposition times when utilizing a 5 wt % TMG solution. This substantiates observations reported from IR analyses of the coatings.

A comparison of atomic composition of the neat TMG precursor with the AP-PECVD coatings shows that the relative ratios of nitrogen to carbon (N/C) in the coatings are 5−8 times less than the TMG. Despite the low uptake on nitrogen-containing groups, the inclusion of nitrogen into the coatings verifies the incorporation of guanidine and its oligomeric fragments into the coatings. High resolution (HR) scans of the C_{1s} curves were used to better understand the incorporation of guanidine-based substituent as well as the oxygen-containing groups.

Deconvolution of the C_{1s} peaks of the TMG coatings on UHMWPE film substrates are shown in Figure 3. The C_{1s} peak of the as-received UHMWPE film (not shown) consists of a

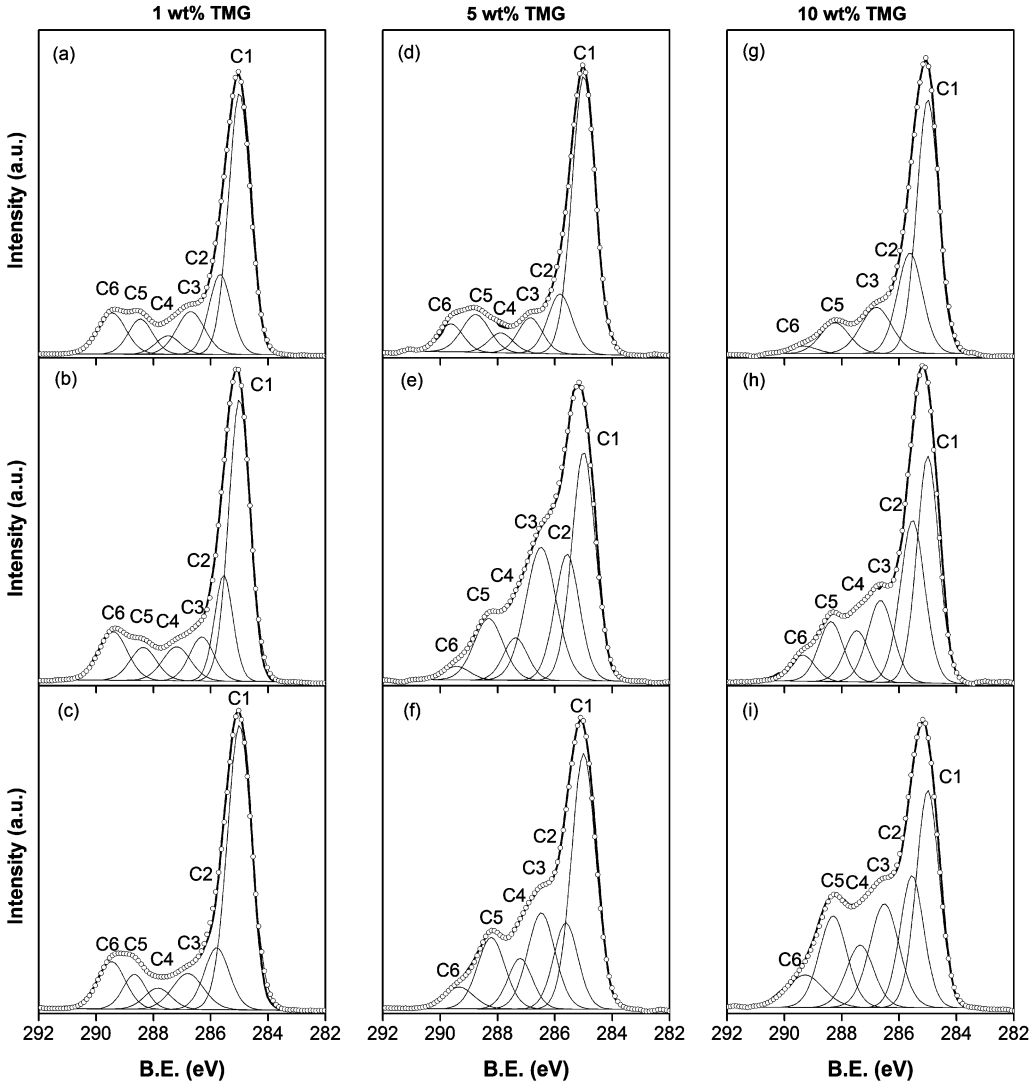

Figure 3. Experimental (—) and peak-fitted (-O-) high resolution C1s curves of UHMWPE films, deposited with (a−c) 1 wt %, (d−f) 5 wt %, and (g−i) 10 wt % TMG in DI water at deposition times of 30 s (top), 60 s (middle), and 180 s (bottom). A full width at half maximum (FWHM) of 1.6 or less was used for peak-fitting.

single, narrow bell curve with a fitted peak at 285.0 eV corresponding to the C−C sp^3 groups. The broadening of the C_{1s} peak and the shifting of the curve's tail towards higher binding energies reconfirm the inclusion of various chemical groups in the coatings as seen from FTIR results. A total of 6 peaks were fitted at different binding energies and assigned to various bonding states of carbon as are given in Table 3.

Table 3. Binding Energies Corresponding to Chemical Groups Identified from Deconvolution of in C_{1s} Spectra[25−27]

	binding energy (eV)	functional group assignment
C1	285.0	C−C, C−H
C2	285.5−285.6	C−N
C3	286.5−286.8	C−O or C═N
C4	287.2−287.6	C═O or N−C−O
C5	288.2−288.7	O═C−N
C6	289.3−289.5	O═C−O, N−CO−N

Peak-fitting results of the HR C_{1s} peaks further support the role of TMG concentration on the chemical composition of the coatings. Coatings grown from 5 and 10 wt % TMG solutions yield C_{1s} curves with a broader tail, especially after deposition times of 60 and 180 s. These coatings tend to have higher concentrations of amine, imine, imide, and amide groups but, in contrast, also hydroxyl and carbonyl groups. Deposition times also influenced the chemistry of the coatings as the concentration of functional groups in coatings varied. This was mainly observed through the amine, amide, and hydroxyl groups as the concentration of these groups increased with deposition time in the 5 and 10 wt % TMG coatings. The highest concentration of the guanidine-based groups, amines, imines, and amides, were found in coatings grown after 60 s and 180 s of exposure to the plasma.

Drawing on the observations from spectroscopic analyses of the coatings, it is speculated that several reaction mechanisms proposed in Scheme 1 occur during the AP-PECVD deposition process. IR data suggest the formation of three major chemical groups, comprised of urea and guanidine functionalities found in the products **III**, **IV**, and **V** in the as-deposited coatings. The two principal mechanisms in operation involve either the abstraction of a methyl group or the abstraction of the imine functionality of the guanidine. The two primary reaction pathways are shown in the scheme, both as the first reaction of the TMG molecule.

In Pathway 1, **II** was generated likely after plasma-induced chain scission of the carbon−nitrogen bond (N−CH_3) of TMG, followed by the addition of atomic hydrogen to the nitrogen radical. Chain scission of a second N−CH_3 group leads to **V** after the addition of atomic hydrogen to the nitrogen radical. Product **IV** is formed from **II** after plasma-induced chain scission of N−CH_3, followed by the subsequent addition of atomic hydrogen to the nitrogen radical.

In Pathway 2, plasma-generated radical exposure of the TMG molecules can lead to the formation of **III** but not **II** or **V** as the initial steps involves the conversion of the C═N group into a C═O group. Hydroxide radical attack of the C═N bond of TMG leads to a transient radical species. The amino radical group can then pick up a hydrogen from water, or abstract the proton intramolecularly, as shown, which subsequently leaves following the formation of the C═O of product **III**. Compound **III** can then undergo a similar reaction path as shown in Pathway 1, which includes a double chain scission of

Scheme 1. Proposed Pathways of Guanidine-Based Radicals Generated in Plasma Interaction

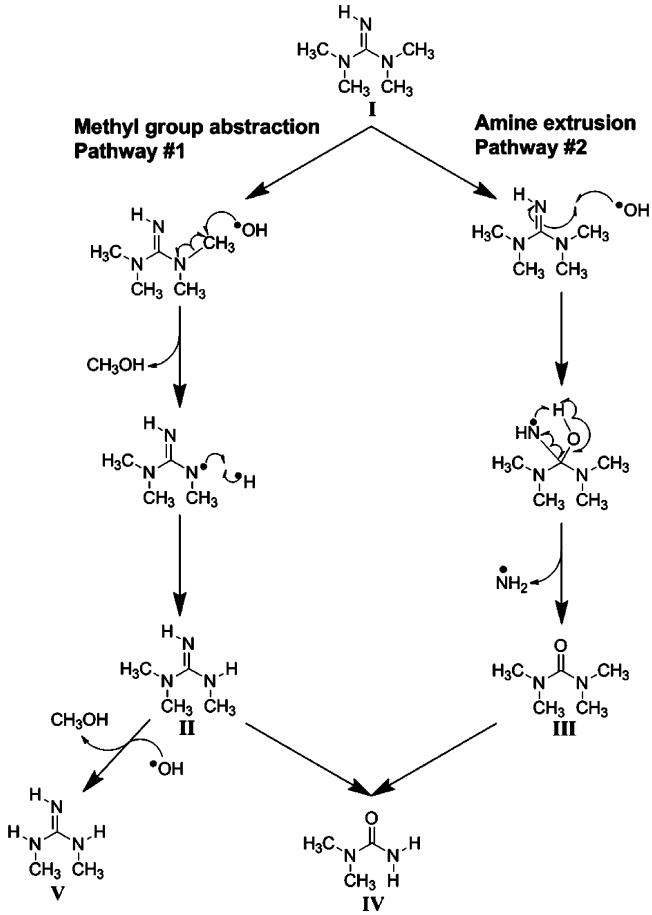

the carbon nitrogen bond (N−CH_3) of **III** followed by hydrogen additions to form **IV**.

It is expected that a large part of the energy transmitted to the plasma is consumed in the form of collisions between the formed radicals and the aforementioned plasma-induced reactive species, leading to energy loss and radical recombination. This effect can significantly lower the density of radicals which are expected to act as "building blocks" for film formation. Another factor taken into consideration in the composition of coatings was the likelihood of the TMG monomer reacting with water prior to plasma interactions. Anderson and Hammer[28] proposed several hydrolysis mechanisms, where two highly plausible products from the reaction yields 1,1-dimethylurea and dimethylamine. Other proposed products include tetramethylguanidinium hydroxide, tetramethylurea, or 1,1-dimethylguanidine. Functional groups found in these products, such as imines, amides, and amines, were identified in the AP-PECVD coatings.

To determine whether the suggested reaction mechanisms were due to hydrolysis or plasma-induced reactions, NMR studies were conducted on the as-prepared 1, 5, and 10 wt % TMG in water solutions. To determine whether a similar reaction was taking place with the aqueous solutions in this study, ^1H and ^{13}C NMR analysis was used to identify possible reaction products. NMR samples were made by mixing 500 μL of deuterated acetone with 100 μL of 1 wt %, 5 wt %, and 10 wt % aqueous TMG solutions. Neat-deuterated acetone, water-deuterated acetone, and TMG-deuterated acetone were also

made to establish the acetone, water, and TMG signals in the ^{1}H NMR spectra. These experiments established that the acetone signal was located at 2.12 ppm, the water signal was located at 4.01 ppm, and TMG at 2.65 ppm. ^{1}H NMR analysis of the TMG solutions suggests that no reaction occurred since no additional peaks other than the TMG, water, and acetone peaks appeared in the spectra. If a reaction would have occurred, additional peaks would be expected if reaction products suggested previously were present. This suggestion is further corroborated by the ^{13}C NMR spectra of the 1%, 5%, and 10% samples, which also does not have any additional peaks besides the TMG peaks. Besides the deuterated acetone peaks, the only peaks present are the C═N peak at 168 ppm and N−CH_3 peaks at 39.5 ppm.

3.2. Structural and Morphological. Representative SEM images (Figure 4) show that there are clear and well-defined features that differentiate the uncoated UHMWPE film from the TMG coated UHMWPE films. Moreover, the effect of TMG concentration and deposition time was illustrated as well. The darker and island-like features correspond to the coating, while the lighter regions correspond to the UHMWPE film substrate in the case of the 1 and 10 wt % TMG coatings. These physical features were measured to be on the order of nanometers and micrometers depending on the concentration of TMG used in the precursor and the deposition time. With longer deposition times and increasing TMG concentrations, these island-like structures grew in size and covered larger areas of the film surface. However, the 5 wt % TMG coatings did not exhibit the features associated with the 1 and 10 wt % TMG coatings. In contrast, elongated oblong-like structures cover the surface of the PE film, indicating a conformal coating of the film was achieved. It is uncertain as to why this particular film growth behavior is observed, but it is believed that the coating distribution or coverage will likely influence antimicrobial performance. To better quantify these structures, AFM was used to image the surface.

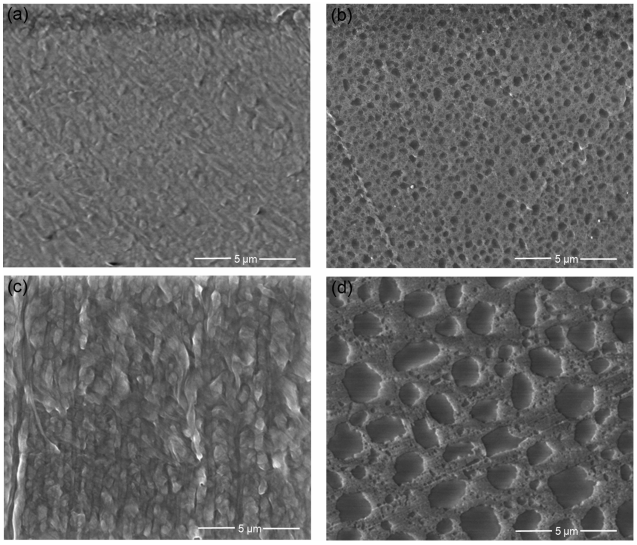

Figure 4. SEM images of the surface topography of (a) untreated UHMWPE film and after a deposition time of 60 s using (b) 1 wt %, (c) 5 wt %, and (d) 10 wt % TMG solution.

Further assessment of the coatings using AFM revealed additional information regarding the role that TMG concentration and deposition times have on the AP-PECVD deposition. These images, shown in Figure 5, corroborate the morphology of the surface imaged by SEM. They also illustrate the addition of new physical features to the surface, where nanometer to micrometer-sized islands were found to have formed uniformly throughout the UHMWPE film. From AFM micrographs, the coating can be described to proceed through different phases in the growth process of the thin film coating and are governed by the concentration of the TMG in the precursor. This observation is clearly depicted from the scanned areas of the coatings formed with 1, 5, and 10 wt % (Figure 5) TMG after 30 s of deposition time. Evaluating the size of these features, the diameter of these islands in the 1 wt % TMG coatings ranged from 100 nm to 1.5 μm, while in the 5 wt % coatings, the diameters spanned from 100 nm to as large as 2 μm. The 10 wt % coatings exhibited features that ranged from 1−4 μm in size.

Due to the inclusion of these features, an increase in surface roughness of the UHMWPE film was measured in comparison to the uncoated UHMWPE film (39 ± 6 nm). Moreover, the roughness was observed to increase further with increasing deposition time. The 1 wt % TMG coatings exhibited surface roughness of 27 ± 6, 50 ± 11, and 61 ± 10 nm after deposition times of 30, 60, and 180 s, respectively. Surface roughness values of the 5 wt % coatings were recorded to be 36 ± 4, 47 ± 5, and 59 ± 4 nm, and the 10 wt % coatings were 52 ± 8, 82 ± 22, and 62 ± 10 nm, after 30, 60, and 180 s, respectively.

The formation of these three-dimensional clusters or islands after initial and prolonged deposition times resemble the Volmer-Weber growth mechanism observed typically with metal-based and semiconductor coatings rather than a layer-by-layer mechanism. This is evident as the coating is not continuous as the formation of the islands is due to stronger interactions between the precursor atoms/molecules (molecular forces) rather than with the substrate surface (surface tension). Similar instances were observed by Michelmore et al.[29] where island structures resulted in the initial plasma-polymerization deposition stages of n-heptylamine, an amine-containing compound. It can be assumed that preferential nucleation of fragmented segments of the monomer at defects and/or reactive sites created from plasma/surface interactions occur during the plasma deposition process. As the deposition process proceeds with longer times, it is likely that these surface structures reach a critical size and coalesce with neighboring structures, thus resulting in larger islands and increased surface roughness or form a continuous film.

3.3. Antimicrobial Performance. Coatings with chemical compositions with the highest atomic concentration of nitrogen-containing species were applied onto woven fabrics to test the antimicrobial behavior of the coatings. Spectra and nylon/cotton woven fabrics were used as the substrate material. Coatings were deposited using 5 and 10 wt % TMG precursor solutions with a deposition time of 60 s. These coatings were evaluated to correlate attributable effects of chemical and physical properties of the coating to overall antimicrobial performance.

Antimicrobial efficiency (as measured by the Sun modification[19] of the AATCC 100 test) of the coating deposited on Spectra varied based on the organisms tested. Spectra with the 5 wt % TMG coating saw a 5% reduction against *E. coli* and no reduction against *S. aureus*, whereas the 10 wt % TMG coating resulted in a 34% reduction for *E. coli* and a 91% reduction of *S. aureus*. The discrepancy in the antimicrobial behavior of the coatings on the Spectra is speculated to have been due to the

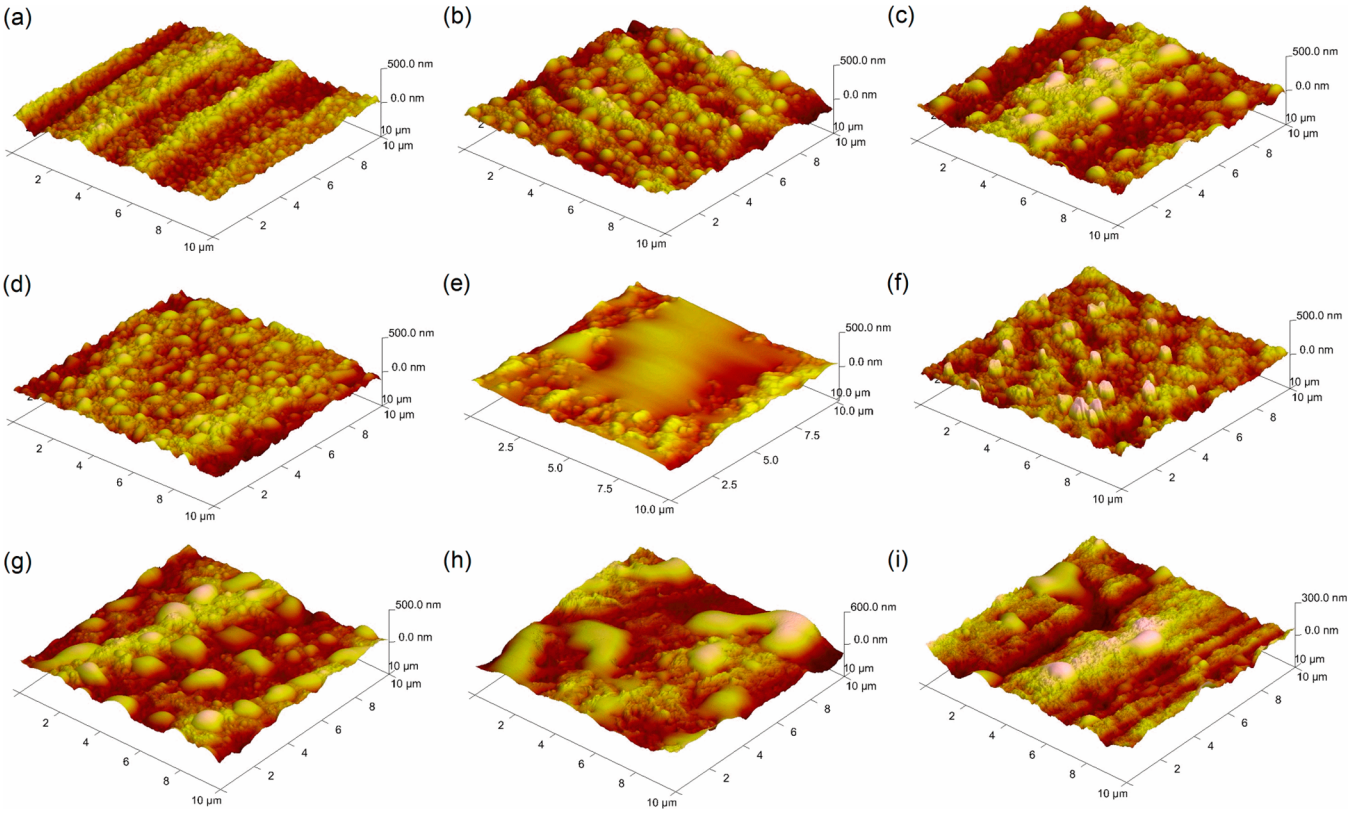

Figure 5. AFM images of (a–c) 1 wt %, (d–f) 5 wt %, and (g–i) 10 wt % TMG coatings deposited on UHMWPE films after 30, 60, and 180 s, respectively. 10 × 10 μm scanned areas.

drying of the inoculum on the uncoated Spectra, owing to its hydrophobicity, thus providing an inaccurate measurement of the bacteria on the coated fabric.

The antimicrobial results of the 5 and 10 wt % TMG coatings on the nylon/cotton fabric are presented in Table 4. Coatings on the nylon/cotton fabric were more effective where 100% bactericidal efficiency with *E. coli* and *S. aureus* were achieved. Moreover, the 5 wt % TMG coating demonstrated a 5 log reduction, while a 3 log reduction was observed with the 10 wt % TMG coating. It is presumed that the cationic and alkaline nature of the guanidine derivative is retained during the plasma deposition process and is the main mechanism in which the coatings exhibit substantial antimicrobial performance (i.e., the film would be highly protonated on contact with an aqueous medium). The difference in the performance between the 5 and 10 wt % coatings could be due to the chemical and/or physical properties of the coatings when applied to a more complex 3D surface. Referring to the XPS atomic concentrations for the 5 and 10 wt % TMG coatings, the latter exhibited 1.2 times less nitrogen-bonded groups indicating that fewer oligomeric chains from the TMG monomer were incorporated into the film.

Table 4. Antimicrobial Performance of Nylon/Cotton Fabric with 5 and 10 wt % TMG Coatings Deposited after 60 s

organism	% TMG (w/w)	bactericidal efficiency (%)
E. coli	control	-
	5	99.999%
	10	99.9%
S. aureus	control	-
	5	99.999%
	10	99.9%

When comparing the performance of the coatings on different woven fabrics, it is speculated that the adhesion between the woven fabric and the antimicrobial coating varies, where in the case of Spectra the adhesion between the coating and the surface can be said to be poorer than in the case of the nylon/cotton. This can bring about partial removal of the coating when the fabric swatches are subjected to the ethanol/water rinse prior to testing, thus leading to a lower than expected antimicrobial performance. This factor warrants additional studies as durability and reusability of the coatings is an important aspect in the application of these coatings, but nonetheless, results indicate that the coatings show promising biocidal activity against both types of bacterial organisms.

4. CONCLUSION

Guanidine-derived antimicrobial coatings were successfully deposited using 1,1,3,3-tetramethylguandine (TMG) through an AP-PECVD method. In general, the study showed that the TMG concentration in the precursor solution and deposition times can have a profound impact on the resultant properties of the coatings. The existence of a polymeric, guanidine-like coating on UHMWPE films was verified from ATR-FTIR and XPS. Notable functional groups identified from spectroscopy include amines, imines, and amides, in addition to hydroxyls, carbonyl, and carboxyl groups. The dependence on the TMG concentration in the precursor solution was seen in the chemical composition of the coatings, where concentration of guanidine-based groups were more prevalent in the 5 and 10 wt % TMG coatings with longer deposition times than in the 1 wt % TMG coatings. In addition to compositional effects, the

morphology of the coatings was affected. SEM and AFM showed evidence of incomplete coverage of the UHMWPE film, where island-like features were observed with the 1 and 10 wt % coatings. These structures were found to gradually grow in size with longer deposition time, resulting in a rougher surface. In contrast, the 5 wt % coatings exhibited a more conformal coating comprised of interconnected oblong-shaped features that covered uniformly throughout the film. Antimicrobial tests of the coatings proved that partial to complete reduction in *E. coli* and *S. aureus* can be realized. The 5 and 10 wt % TMG coatings show potential as effective antimicrobial agents that can be applied to polymeric substrates. It can be assumed that the variations in the antimicrobial performance can be a result of the chemistry and physical characteristics of the coatings. Overall, it has been demonstrated that AP-PECVD can produce coatings with promising antimicrobial performance when appropriate deposition conditions are applied.

AUTHOR INFORMATION

Corresponding Author

*Phone: +1 410-306-3307. Fax: +1 410-306-0829. E-mail: victor.rodriguez31@us.army.mil.

Author Contributions

The manuscript was written through contributions of all authors. All authors have given approval to the final version of the manuscript.

Notes

The authors declare no competing financial interest.

ACKNOWLEDGMENTS

We thank Dr. Joshua Orlicki for his help with the proposed mechanism of TMG deposition. This research was supported in part by an appointment to the Postgraduate Research Program at the U.S. Army Research Laboratory administered by the Oak Ridge Institute for Science and Education through an interagency agreement between the U.S. Department of Energy and USARL.

REFERENCES

(1) Paulus, W. *Directory of Microbicides for the Protection of Materials A Handbook*; Springer-Verlag: New York, 2005; pp 9−23.
(2) Weinberg, E. D. *Ann. N. Y. Acad. Sci.* **1968**, *148*, 587−600.
(3) Buxbaum, A.; Kratzer, C.; Graninger, W.; Georgopoulos, A. *J. Antimicrob. Chemother.* **2006**, *58*, 193−197.
(4) Kaehn, K. *Skin Pharmacol. Physiol.* **2010**, *23*, 7−16.
(5) Qian, L.; Li, X.; Sun, S.; Xiao, H. J. *Biobased Mater. Bioenergy* **2011**, *5*, 219−224.
(6) Rosenthal, I.; Juven, B. J.; Ben-hur, E. *J. Food Saf.* **1982**, *4*, 191−197.
(7) Zhang, Y.; Jiang, J.; Chen, Y. *Polymer* **1999**, *40*, 6189−6198.
(8) Qian, L.; Xiao, H.; Zhao, G.; He, B. *ACS Appl. Mater. Interfaces* **2011**, *3*, 1895−1901.
(9) Bromberg, L.; Hatton, T. A. *Polymer* **2007**, *48*, 7490−7498.
(10) Ratner, B. D. *J. Biomater. Sci., Polym. Ed.* **1993**, *4*, 3−11.
(11) Kumar, V.; Pulpytel, J.; Rauscher, H.; Mannelli, I.; Rossi, F.; Arefi-Konsari, F. *Plasma Processes Polym.* **2010**, *7*, 926−938.
(12) Vasudev, M. C.; Anderson, K. D.; Bunning, T. J.; Tsukruk, V. V.; Naik, R. R. *ACS Appl. Mater. Interfaces* **2013**, *5*, 3983−3994.
(13) Vartiainen, J.; Tuominen, M.; Na, K. *J. Appl. Polym. Sci.* **2010**, *116*, 3638−3647.
(14) Gawish, S. M.; Matthews, S. R.; Wafa, D. M.; Breidt, F.; Bourham, M. A.; Carolina, N. *J. Appl. Polym. Sci.* **2005**, *103*, 1900−1910.
(15) Bazaka, K.; Jacob, M. V.; Truong, V. K.; Wang, F.; Arachchilage, W.; Pushpamali, A.; Wang, J. Y.; Ellis, A. V.; Berndt, C. C.; Crawford, R. J.; Ivanova, E. P. *Biomacromolecules* **2010**, *11*, 2016−2026.
(16) Chen, G.; Zhou, M.; Zhang, Z.; Lv, G.; Massey, S.; Smith, W.; Tatoulian, M. *Plasma Processes Polym.* **2011**, *8*, 701−708.
(17) Sarghini, S.; Paulussen, S.; Terryn, H. *Plasma Processes Polym.* **2011**, *8*, 59−69.
(18) Davis, R.; El-Shafei, A.; Hauser, P. *Surf. Coat. Technol.* **2011**, *205*, 4791−4797.
(19) Sun, Y.; Sun, G. *J. Appl. Polym. Sci.* **2003**, *88*, 1032−1039.
(20) Liu, D. X.; Bruggeman, P.; Iza, F.; Rong, M. Z.; Kong, M. G. *Plasma Sources Sci. Technol.* **2010**, *19*, 025018.
(21) Rodriguez-Santiago, V.; Bujanda, A. A.; Stein, B. E.; Pappas, D. D. *Plasma Processes Polym.* **2011**, *8*, 631−639.
(22) Socrates, G. *Infrared and Raman Characteristic Group Frequencies: Tables and Charts*, 3rd ed.; John Wiley & Sons, Ltd.: Chichester, UK, 2001; pp 1−347.
(23) Smith, B. C. *Infrared Spectral Interpretation: A Systematic Approach*; CRC Press LLC: Boca Raton, FL, 1999; pp 31−146.
(24) Adhikari, R.; Dao, B.; Hodgkin, J.; Mardel, J. *Eur. Polym. J.* **2011**, *47*, 1328−1337.
(25) Shard, A. G.; Whittle, J. D.; Beck, A. J.; Brookes, P. N.; Bullett, N. A.; Talib, R. A.; Mistry, A.; Barton, D.; McArthur, S. L. *J. Phys. Chem. B* **2004**, *108*, 12472−12480.
(26) Truica-Marasescu, F.; Wertheimer, M. R. *Plasma Processes Polym.* **2008**, *5*, 44−57.
(27) Briggs, D. *Surface Analysis of Polymers by XPS and Static SIMS*; Cambridge University Press: Cambridge, UK, 1998; pp 47−87.
(28) Anderson, M. L.; Hammer, R. N. *J. Chem. Eng. Data* **1967**, *12*, 442−447.
(29) Michelmore, A.; Martinek, P.; Sah, V.; Short, R. D.; Vasilev, K. *Plasma Processes Polym.* **2011**, *8*, 367−372.